2019

In Situ Monitoring of Linear RGD-Peptide Bioconjugation with Nanoscale Polymer Brushes

Evmorfia Psarra
Leibniz Institute of Polymer Research Dresden

Ulla Konig
Leibniz Institute of Polymer Research Dresden, koenig-ulla@ipfdd.de

Martin Muller
Leibniz Institute of Polymer Research Dresden

Eva Bittrich
Leibniz Institute of Polymer Research Dresden

Klaus-Jochen Eichhorn
Leibniz Institute of Polymer Research Dresden

See next page for additional authors

ACS OMEGA

Article

http://pubs.acs.org/journal/acsodf

In Situ Monitoring of Linear RGD-Peptide Bioconjugation with Nanoscale Polymer Brushes

Evmorfia Psarra,[†,§,∥] Ulla König,*[,†,∥] Martin Müller,[†] Eva Bittrich,[†] Klaus-Jochen Eichhorn,[†] Petra B. Welzel,[†] Manfred Stamm,[†,‡] and Petra Uhlmann*[,†,§]

[†]Leibniz Institute of Polymer Research Dresden, Hohe Street 6, 01069 Dresden, Germany

[‡]Faculty of Science, Department of Chemistry, Chair of Physical Chemistry of Polymeric Materials, Technische Universität Dresden, Bergstr. 66, 01069 Dresden, Germany

[§]Department of Chemistry, Hamilton Hall, University of Nebraska-Lincoln, 639 North 12th Street, Lincoln, Nebraska 68588, United States

ABSTRACT: Bioinspired materials mimicking the native extracellular matrix environment are promising for biotechnological applications. Particularly, modular biosurface engineering based on the functionalization of stimuli-responsive polymer brushes with peptide sequences can be used for the development of smart surfaces with biomimetic cues. The key aspect of this study is the in situ monitoring and analytical verification of the biofunctionalization process on the basis of three complementary analytical techniques. In situ spectroscopic ellipsometry was used to quantify the amount of chemisorbed GRGDS at both the homopolymer poly(acrylic acid) (PAA) brush and the binary poly(*N*-isopropylacrylamide) (PNIPAAm)−PAA brushes, which was finally confirmed by an acidic hydrolysis combined with a subsequent reverse-phase high-performance liquid chromatography analysis. In situ attenuated total reflection-Fourier transform infrared spectroscopy provided a step-by-step detection of the biofunctionalization process so that an optimized protocol for the bioconjugation of GRGDS could be identified. The optimized protocol was used to create a temperature-responsive binary brush with a high amount of chemisorbed GRGDS, which is a promising candidate for the temperature-sensitive control of GRGDS presentation in further cell-instructive studies.

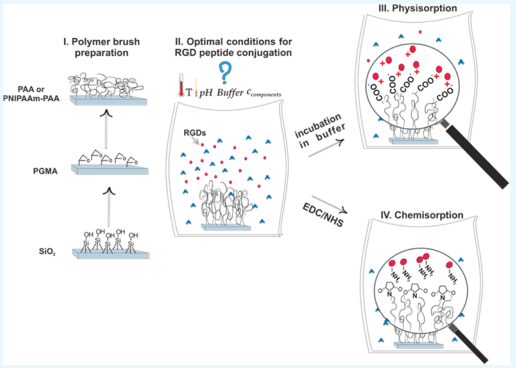

1. INTRODUCTION

Advanced engineered biosurfaces have to not only recognize but also modulate complex molecular biointerfacial processes occurring in biological microenvironments. The current biomimetic surface engineering strategies have been developed to create graded and adaptive synthetic biointerfaces with multiple stimuli-sensitive functions able to modify their interactions with cells and biomolecules. In this regard, surface bioengineering approaches for various biotechnological and biomedical applications especially focus on the creation of biomimetic substrates that resemble the ECM microenvironment. For instance, engineering cell adhesion onto surfaces is often mediated by short peptide sequences (integrins), which specifically bind to intracellular membrane proteins.[1] Because the RGD (Arg-Gly-Asp) tripeptide motif is one of the most common minimal-recognition sequences for integrin receptors, various surface biofunctionalization approaches have been employing the introduction of RGD-containing moieties by various biofunctionalization strategies.[2,3] For cell adhesion at bioengineered surfaces, longer synthetic oligopeptides, such as GRGDS (Gly-Arg-Gly-Asp-Ser) or GRGDSPK (Gly-Arg-Gly-Asp-Ser-Pro-Lys), can be applied to elicit cellular impacts similar to those of native ECM proteins.[4−6]

In recent years, advanced nanocoatings have attracted great attention. A special method to create such ultrathin coatings is tethering stimuli-responsive polymers by one functional terminal group onto a surface. If the surface-grafting density is high enough, the polymer chains are forced to stretch away from the interface due to excluded volume effects, creating a polymer brush. Nanoscale polymer brushes are advantageous because of their well-defined constitution and synergistic response to external stimuli. Therefore, polymer brushes exhibit effective nanostructures and have the promising potential to regulate complex interactions even in natural living systems. Polymer brushes with various chemical compositions have been used to generate responsive thin films on a variety of surfaces.[7−9] Upon switching by external stimuli, biomodified binary brush surfaces can hide or expose biofunctionalities on demand.

One of the most commonly used bioconjugation methods is a carbodiimide-mediated reaction for direct conjugation of carboxylic groups (−COOH) with primary amines ($-NH_2$).[10,11] *N*-Ethyl-*N*′-(3-(dimethylamino)propyl) carbodii-

Received: December 1, 2016
Accepted: February 24, 2017
Published: March 16, 2017

DOI: 10.1021/acsomega.6b00450
ACS Omega 2017, 2, 946−958

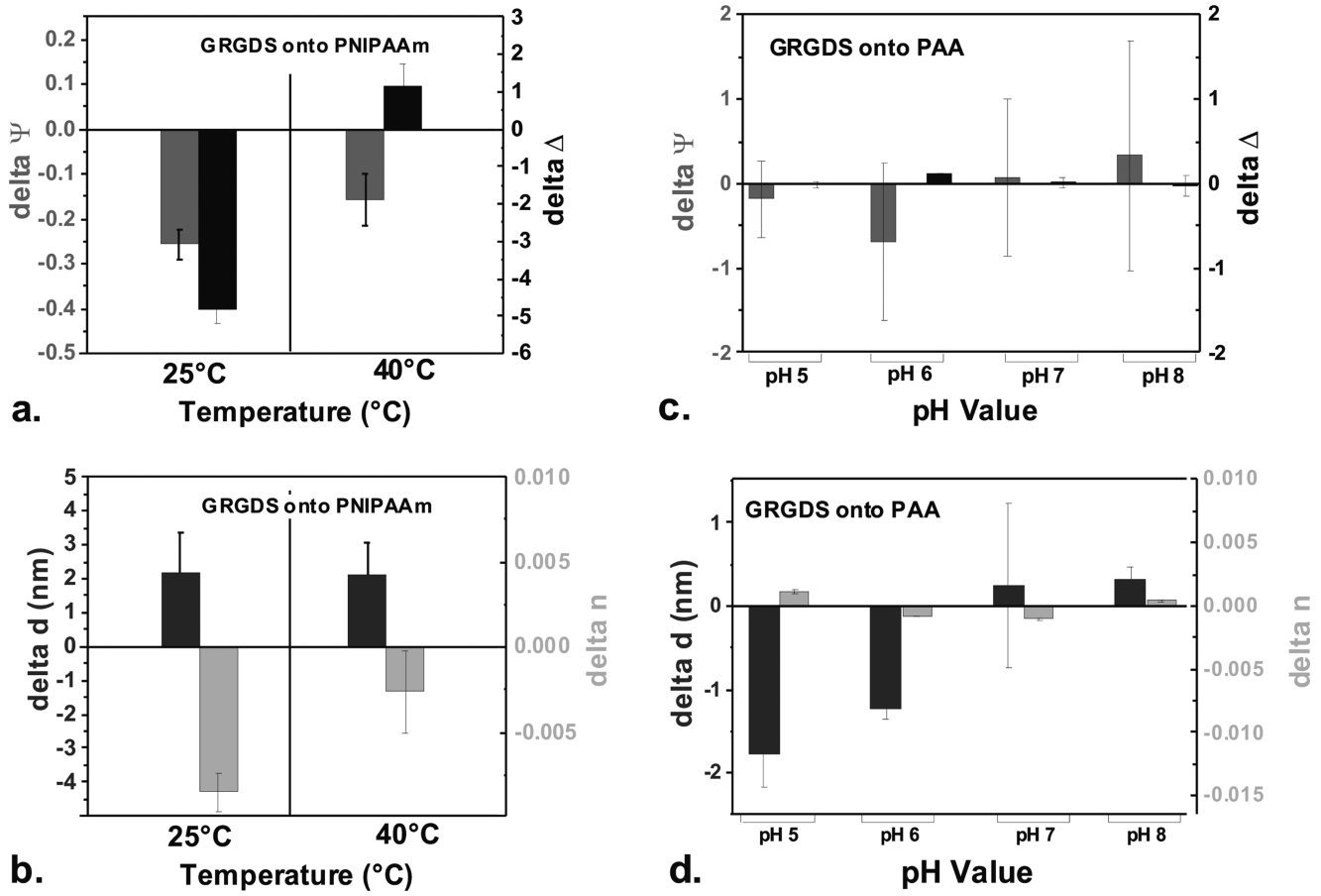

Figure 1. GRGDS physisorption (concentration, 0.1 mg/mL): (a) and (b) onto homo-PNIPAAm brushes at two different temperatures (25 and 40 °C) in PBS buffer and (c) and (d) onto homo-PAA brushes at different pH values using 100 mM sodium acetate (pH 4 and 5) and sodium phosphate (pH 7 and 8) buffers. The change in the ellipsometric angles, Psi (Ψ) and Delta (Δ), for the selected wavelength of 632 nm as well as the changes of thickness (d) and refractive index (n) upon GRGDS-peptide physisorption are plotted vs temperature and pH.

mide (EDC) and *N*-hydroxysuccinimide (NHS) are used simultaneously to increase the reaction efficiency and create stable intermediates.[12−14] The advantages of the EDC/NHS bioconjugation method are its feasibility, high conversion efficiency, and the minor influence on the bioactivity of the conjugated biomolecules due to the mild reaction conditions, as well as the water solubility of the reagents. Moreover, EDC/NHS coupling yields sustainable, nontoxic products compared to other coupling procedures, such as glutaraldehyde and formaldehyde.[15,16] Despite the popular use of the EDC/NHS bioconjugation procedure, only few publications are focusing on the detailed analytical investigation of the carboxyl-to-amine conjugation reaction taking place directly at the interface of nanoscale polymer brush films.[11,13,17−23]

We prepared "grafting-to" brushes of a temperature-responsive polymer, that is, poly(*N*-isopropylacrylamide) (PNIPAAm) with a lower critical solution temperature (LCST) around 32 °C, and poly(acrylic acid) (PAA). PAA contains carboxylic groups, which can be used for covalent binding reactions with amino groups of biomolecules. Biofunctionalization of the polymer brushes with cell-mediating RGD peptides was done by covalent binding (chemisorption) to a PAA homopolymer brush and a more complex thermoresponsive PNIPAAm−PAA binary polymer brush, and related to physisorption. The main objective of this study was the in situ investigation of the stepwise RGD-peptide bioconjugation at these polymer brushes and in the aqueous environment to identify optimal process conditions. For this purpose, complementary high-sensitive in situ attenuated total reflectance Fourier transform infrared spectroscopy (ATR-FTIR), in situ ellipsometry, and acidic hydrolysis combined with a subsequent reverse-phase high-performance liquid chromatography (HPLC) analysis were applied.

2. RESULTS AND DISCUSSION

2.1. Polymer Brush Characterization. As the initial step of our bioconjugation approach, homogeneous nanoscale homo-PAA and homo-PNIPAAm brushes and binary PNIPAAm−PAA brushes with a ratio of 80:20 and 20:80 were prepared. First of all, thin unmodified polymer brush layers were characterized by ellipsometry. Thereby, the following brush thickness values in the dry state were measured: d = 7.2 ± 0.3 nm for the PAA homopolymer brush, d = 9.3 ± 0.3 nm for the PNIPAAm homopolymer brush, and d = 7.2 ± 0.3 nm for the 20:80 PNIPAAm−PAA polymer ratio, as well as d = 12.6 ± 0.4 nm for the 80:20 PNIPAAm−PAA polymer ratio.

In addition to already published information obtained by ATR-FTIR about the *grafting-to* process of PAA brushes[24,25] in Figure 3a, the bottom ATR-FTIR spectrum (I) represents the grafted PAA layer recorded after the *grafting-to* process. Significantly, the ν(C═O) band at 1710 cm^{-1} was obtained, which is indicative of the carboxyl groups of PAA. In Figure 3b, the bottom ATR-FTIR spectrum (I) shows the grafted

DOI: 10.1021/acsomega.6b00450
ACS Omega 2017, 2, 946−958

Scheme 1. Bioconjugation Procedure of Homo-PAA Brush via EDC/NHS Chemisorption[a,b]

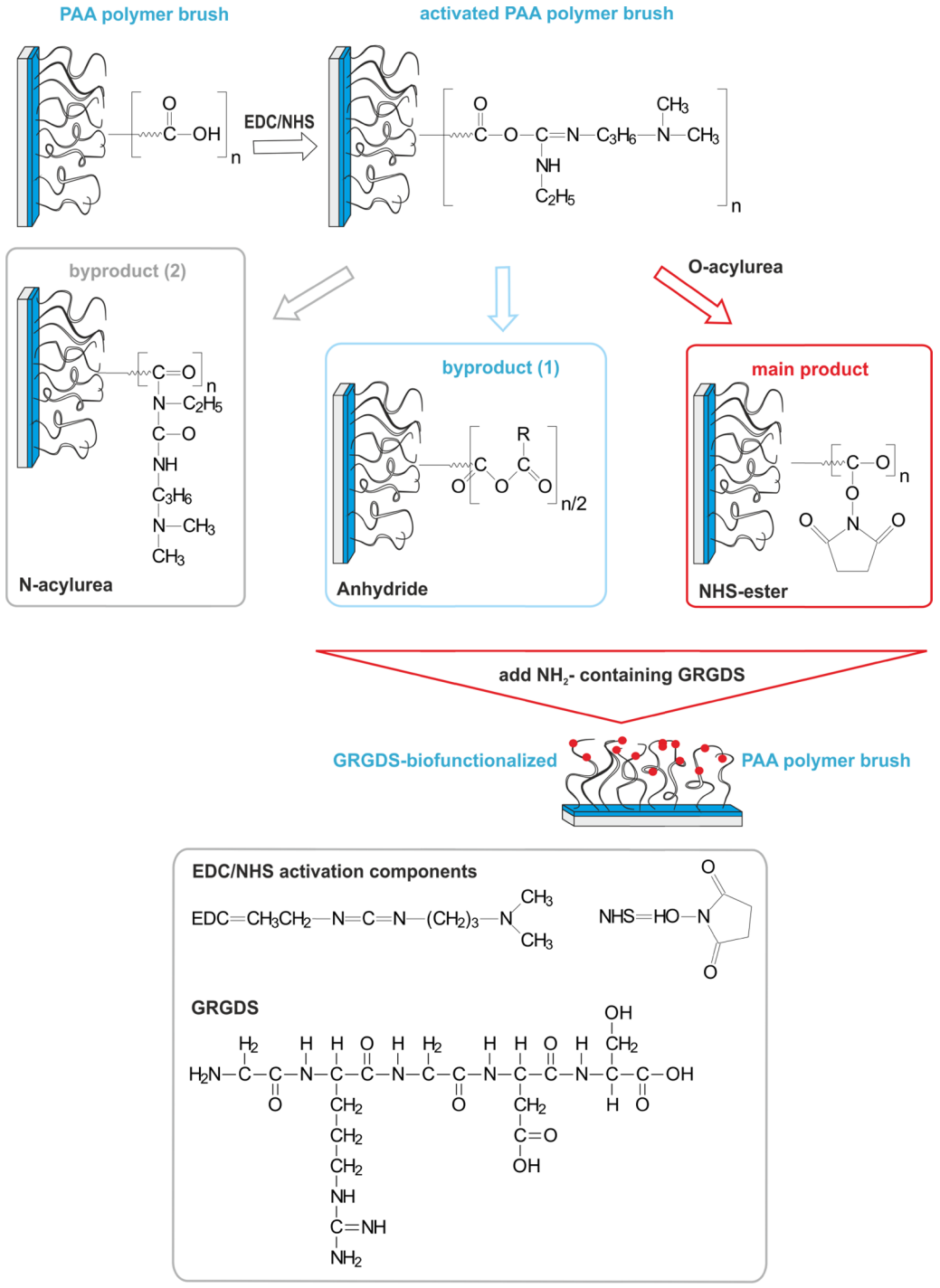

[a]The first formed intermediate, *O*-acylurea, of the EDC/NHS activation is able to react in different ways depending on the reaction conditions. [b]The main product is NHS-ester. By hydrolysis of *O*-acylurea, the COOH functionalities will be regenerated. Further byproducts are the anhydride and *N*-acylurea. Both NHS-ester and the anhydride are reactive toward NH_2-containing biomolecules (herein RGD peptide: GRGDS) and result in covalent binding of the biomolecule to the PAA brush surface by amide formation mainly between the primary amine at the free N-terminus of the peptide, that is, on the glycine residue and the activated ester groups at the PAA. Although GRGDS has a second amine group as part of the guanidinium side group of the arginine amino acid, the primary amine on the glycine residue is expected to be more nucleophilic and more reactive.

PNIPAAm layer with its characteristic amide I and amide II bands at 1630 and 1535 cm^{-1}, respectively.

2.2. Physisorption of GRGDS Peptide onto PNIPAAm and PAA Homopolymer Brushes. The physical adsorption of GRGDS onto PNIPAAm and PAA homopolymer brushes was monitored by in situ spectroscopic ellipsometry. Figure 1a,b shows changes in the ellipsometric angles, swollen thickness, and refractive index upon physisorption of GRGDS onto thermoresponsive PNIPAAm homopolymer brushes. The experiments were performed in phosphate-buffered saline (PBS) (pH 7.4, 100 mM) aiming at physiological conditions and using 0.1 mg/mL GRGDS. Previous investigations of

DOI: 10.1021/acsomega.6b00450
ACS Omega 2017, 2, 946−958

Table 1. EDC/NHS Chemisorption of GRGDS Peptide onto Homo-PAA Brush Surfaces[a,b]

	ACTIVATION		COVALENT BINDING		
Protocol	Solution	EDC/NHS Ratio	Solution	T	Time
Prot. I	DMSO	2.5/1	PBS (pH 7.4)	4°C	16h
Prot. II	Phosphate (pH 6)	2.5/1	PBS (pH 7.4)	4°C	16h
Prot. III	MES (pH 6)	2.5/1	PBS (pH 7.4)	4°C	16h
Prot. IV	MES (pH 6)	1/2.5	PBS (pH 7.4)	4°C	16h
Prot. V	MES (pH 6)	1/2.5	Borate (pH 8.0)	4°C	16h
Prot. VI	MES (pH 6)	1/2.5	Borate (pH 8.0)	25°C	2h
Prot. VII	MES (pH 6)	1/2.5	Borate (pH 8.0)	25°C	16h

[a]Experimental parameters of the final bioconjugation Protocols I–VII. [b]The colors used for each protocol are identical with those used in the figures of ATR-FTIR (Figures 2 and 3), VIS–SE (Figures 4 and 5), and HPLC (Figure 6) analyses.

protein adsorption on PNIPAAm brushes employing the *grafting-to* method showed that PNIPAAm is protein-repellent at 25 °C, whereas only minor amounts of protein were adsorbing at 37 °C.[26,27] Nevertheless, to the best of the authors' knowledge, there are no reported data of RGD-peptide adsorption on these particular PNIPAAm polymer layers. Looking at the change of the ellipsometric angles, Δ and Ψ, before and after GRGDS physisorption, we observed changes, ranging from 0.1 to 0.3° for Ψ and 1 to 5° for Δ (Figure 1a). Error bars are given due to statistical variation over three to six different samples. By fitting of the very sensitive changes in the ellipsometric angles, we obtained negative changes of the refractive index ($|\Delta n| < 0.01$, $\Delta n < 0$) of the swollen layers, for GRGDS physisorption at both temperatures (Figure 1b). These negative changes in n were accompanied by small positive changes in the layer thickness ($\Delta d \sim 1-3$ nm), which can be explained by polymer chain reorientation after peptide incubation and washing (Figure 1b). Modeling of the RGD-peptide surface density, Γ_{RGD}, according to eq 1, led to $\Gamma_{RGD} \sim 0$ mg/m^2, for GRGDS at both temperatures. Considering the particular sensitivity of ellipsometry toward adsorbed amounts higher than 0.5 mg/m^2 at PNIPAAm brushes, it can be concluded that GRGDS physisorption is less than this detection limit at PNIPAAm homopolymer brushes under physiological (i.e., in PBS at pH 7.4) conditions below and above the LCST of the PNIPAAm brushes at 31 °C in PBS buffer.[28]

Further, we performed pH-dependent physisorption experiments on PAA homopolymer brushes. Figure 1c,d shows results of the GRGDS-peptide adsorption at room temperature. According to previously published data, these polyelectrolyte (PEL) brushes are expected to adsorb biomolecules like proteins (e.g., albumin or fibrinogen) in large amounts, which are significantly dependent on salt concentration and pH.[29−32] At high salt concentrations, charges are screened and therefore electrostatic interactions between charged biomolecules and oppositely charged PEL brushes are rather low.[27] On the contrary, high adsorbed amounts of biomolecules are expected at pH values close to the IEP of the biomolecule.[32] We performed GRGDS physisorption at 100 mM ionic strength and at four different pH values (Figure 1c,d): at pH = 5, which is below the IEP of the GRGDS peptide ($pI_{GRGDS} = 6.2$); at pH = 6, which is close to pI_{GRGDS}; at pH = 7; and far above the pI_{GRGDS} at pH = 8, where both the peptide and the surface are negatively charged. Changes in the modeled parameters, d and n, were small, and all adsorbed amounts calculated with eq 1 were below 0.2 mg/m^2. However, the errors of the changes in the original ellipsometric angle (Ψ) are critically large for pH 6–8. The error is calculated by averaging the results for six different samples. Although only minimal adsorption at the PAA brushes occurred at pH 5 under electrostatically attractive conditions, the absence of physisorption at a higher pH remains inconclusive due to statistical variance. However, the absence of significant physisorption at pH 8 in 100 mM borate buffer was

DOI: 10.1021/acsomega.6b00450
ACS Omega 2017, 2, 946−958

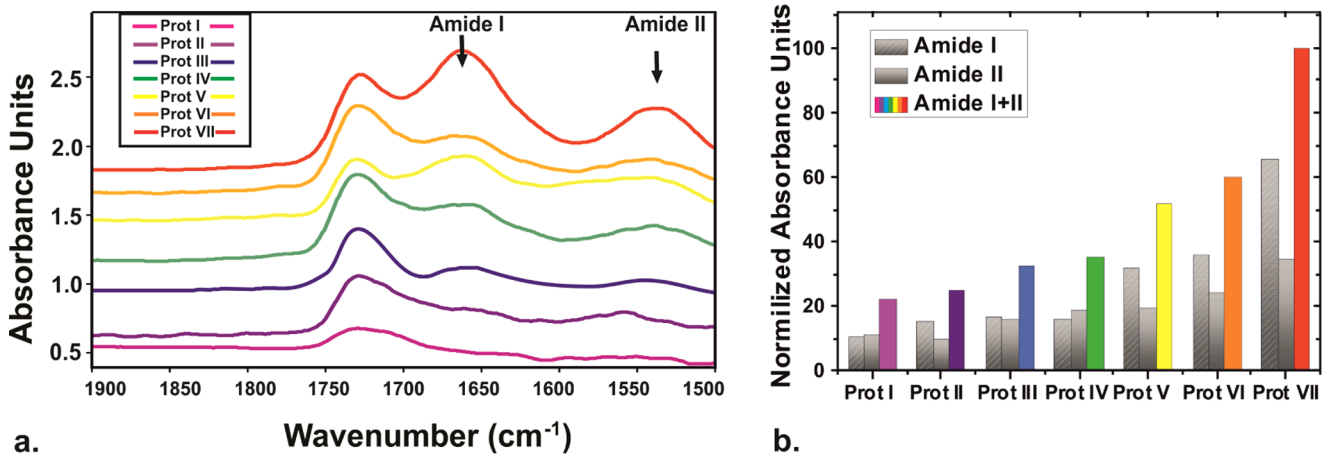

Figure 2. ATR-FTIR analysis of GRGDS bioconjugation (0.1 mg/mL) onto homo-PAA brush surfaces. Comparison of exemplarily selected EDC/NHS chemisorption protocols according to Table 2. (a) Final surface state after GRGDS chemisorption. Curves were shifted along the vertical axis for better display. Rinsing with acetate solution of pH 4.0 was performed before the analysis. (b) Absorbance units refer to normalized relative band intensities of the amide I and amide II as well as the sum of the amide I and amide II vibration frequency bands.

confirmed by acidic hydrolysis and a subsequent HPLC analysis (Figure 6).

In summary, we could confirm that both homopolymer brushes PNIPAAm and PAA do not adsorb the GRGDS peptide in significant amounts relevant for the following chemisorption conditions. For binary brushes, again the HPLC analysis confirmed the absence of significant physisorption (Figure 6). Therefore, to be able to provide end-grafted, nanoscale polymer brushes for specific bioapplications under physiological conditions, there is the need to introduce covalent binding methods, which will be subsequently described.

2.3. Modalities of GRGDS Peptide Bioconjugation Using EDC/NHS on Homo-PAA Brushes. As the next step, to fabricate cell-instructive homo-PAA brushes, GRGDS was chemisorbed onto equilibrated swollen homo-PAA brushes. Herein, GRGDS was covalently bound to the PAA brush surface via carbodiimide conjugation using EDC and NHS simultaneously.

Scheme 1 illustrates the molecular mechanism of GRGDS bioconjugation via EDC/NHS chemisorption. In the first reaction step, an *O*-acylurea intermediate is formed by the reaction of EDC with the carboxylic groups of the PAA brush. Because the formed *O*-acylurea product is prone to hydrolysis in aqueous solution, adding NHS simultaneously to the activation solution can achieve a more stable conversion to the next intermediate. Consequently, NHS-ester as the main product is formed by a nucleophilic attack of NHS to O-acylurea, which can ideally exhibit a very high yield efficiency as shown by Sam et al.[23] However, few other side products may be formed during the activation procedure, for instance, an anhydride probably due to the regeneration of COOH after hydrolysis.[20] The anhydride might further react directly with primary amines and form equal amounts of amide bonds. Furthermore, a stable *N*-acylurea might be formed after intramolecular acyl rearrangements. However, under the reaction conditions applied in our experiments, this is negligible because it only becomes important at high temperatures and high reactant concentrations. Moreover, the reactivity of NHS-ester is highly dependent on pH, which is attributed to different degrees of the protonation of the amine groups. Furthermore, the adjacent amino acids have also an impact on the reactivity of NHS-ester. Although primary amines are most likely to form NHS-ester, other groups present in peptide side chains (−OH for tyrosine, serine, threonine; guanidinium for arginine; and sulfhydryls for cysteines) might also react. Conclusively, it should be noted that the buffer pH of the bioconjugation reaction has to be controlled precisely to favor the N-terminal reaction versus side-chain reactions of the peptides.[20−23,33]

Because of the complexity of the illustrated bioconjugation reaction, our investigation aimed at the optimization of the GRGDS chemisorption process. First of all, a set of seven selected bioconjugation protocols based on the activation and covalent binding methods listed in Table 1 was established. Details of the particular protocols (Prot. I−Prot. VII) are summarized in Table 1. As surface chemical analytical tool, in situ ATR-FTIR spectroscopy was used. ATR-FTIR spectra of the GRGDS-functionalized PAA brush can be found in Figure 2a. The quantitative analysis was based on amide I and amide II band integrals, which can be used as a direct measure of the bound GRGDS amount if the polymer layer is sufficiently thin (d < 100 nm). A similar analytical approach has been reported.[34−36] Determined amide band integrals are given in Figure 2b, illustrating and comparing the different GRGDS bioconjugation efficiencies. The initial GRGDS concentration was 0.1 mg/mL for all experiments.

Concerning the activation step, for an optimal GRGDS conjugation efficiency, several factors, such as solvent, pH, and the control of competitive side reactions, have to be considered. Alternatively to aqueous solutions, dimethyl sulfoxide (DMSO) is often used to dissolve EDC/NHS. Thereby, the hydrolysis of the intermediate products can be avoided.[37] Protocol I refers to the GRGDS conjugation after activation in DMSO. Figure 2b shows low amide I and amide II band integrals, indicating low amounts of immobilized GRGDS. In this case, the covalent binding of GRGDS to the PAA brush was insufficient. Therefore, buffer solutions were used for the following protocols.

The EDC reaction is most efficient under slightly acidic (pH 5−6) conditions and must be performed in carboxyl- and amine-free buffers.[37,38] In Figure 2, Protocol II shows results for phosphate buffer at pH 6. It is known that the dissociation of carboxylic groups is advantageous for an effective COO^- turnover to the *O*-acylurea intermediate.[22,39] Attendant, in situ ellipsometric analysis has shown a considerably stronger

DOI: 10.1021/acsomega.6b00450
ACS Omega 2017, 2, 946−958

Table 2. Infrared Band Assignments in the Carbonyl Stretching Frequency Region[44]

wavenumber (cm^{-1})	vibration mode	molecular assignment
1729	ν (C═O), carbonyl stretching	poly(glycidyl methacrylate) (PGMA) (dry), ester
1713	ν (C═O), carbonyl stretching	PAA (dry), COOH
1720	ν (C═O), carbonyl stretching	PAA (in situ), COOH
1556	ν_a(C═O), assymm. stretching	PAA (in situ), COO^-
1800	ν (C═O), carbonyl stretch	NHS-ester
1761	ν_s (C═O), imidyl symmetric stretching	NHS-ester
1732	ν_{as} (C═O), imidyl assymmetric stretching	NHS-ester, C═O
1660	amide I, mainly ν(C), C═O stretching	RGD, amide groups
1550	amide II, mainly δ(N−H), N−H bending	RGD, amide groups

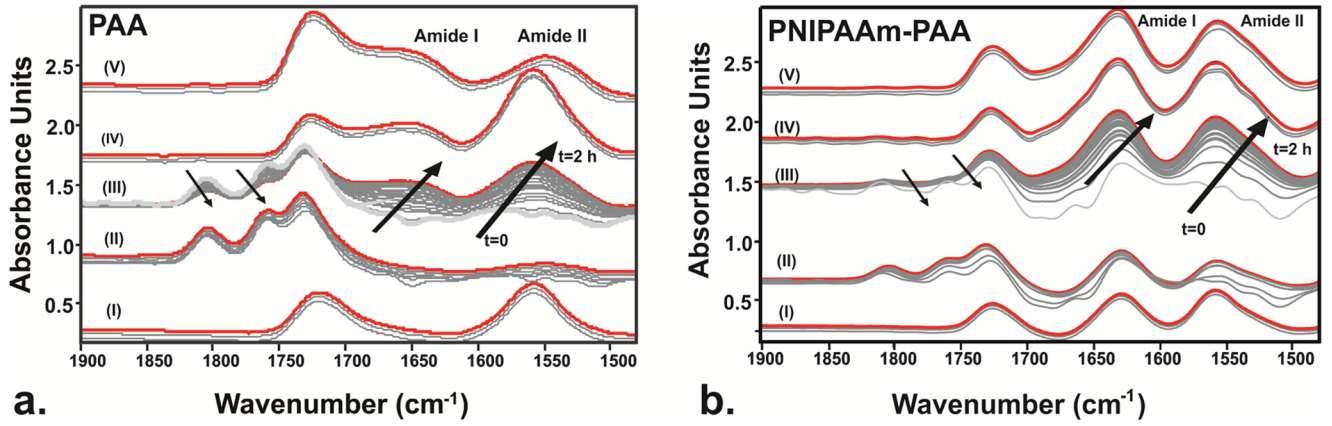

Figure 3. In situ ATR-FTIR spectra of GRGDS bioconjugation (0.1 mg/mL) onto polymer brushes. (a) GRGDS covalent binding to PAA brush; (b) GRGDS covalent binding to PNIPAAm−PAA brush with a ratio of 80:20. The experiment was performed in five discrete steps. Step I: swelling of the brush in MES; step II: EDC/NHS activation; step III: GRGDS conjugation; step IV: washing with PBS; and step V: quenching with acetate buffer at pH 4.0. The spectra were dynamically recorded over the entire time frame of each experimental step with a time step of t = 5 min. Curves were shifted along the vertical axis for better display.

swelling of the brush layer at pH 6 due to a larger degree of dissociation of the COOH groups of the brush (data not shown). The ionic strength of all used buffers was kept constant at 100 mM. Comparing Protocol II with Protocol III, for which 2-(*N*-morpholino)ethanesulfonic acid (MES) buffer was used instead of phosphate buffer during the activation step, we could see an 8% increase in amide I + amide II intensities. This could be explained by the fact that EDC can be slightly reactive toward phosphate groups, which act as competitive inhibitors in the very first step of the activation procedure.[37] An increase in the concentration of EDC could alternatively solve this problem.

One main consideration that should be taken into account concerning the covalent binding reaction step is the competition between the NHS-ester hydrolysis and the reaction with primary amines. The half-life of NHS-ester strongly depends on the reaction temperature and the pH of the buffer solution. Because the existence of hydroxyl ions promotes the hydrolysis of NHS-ester, pH > 8 is not preferable. A comparison of Protocols IV and V (Figure 2) shows the *influence of the specific buffers*, PBS (pH 7.4) and borate (pH 8.0), applied in the final covalent conjugation step. An increase in amide I + amide II intensities of around 16% was observed here. Therefore, as for various other published protocols, the use of borate buffer was proved to be beneficial compared to that of PBS during GRGDS-peptide chemisorption.[37,40−42]

The *variation of the molar ratio of EDC to NHS* had only a minor influence on the conjugated GRGDS amount. Protocol III showed an increase of about 3% in amide I + amide II intensities of compared to that of Protocol IV, where 1 mM EDC and 2.5 mM NHS dissolved in MES buffer solution (pH 6, 100 mM) were employed.

Along with the effect of the pH value on the NHS-ester lifetime, the selected conjugation temperature is an important parameter. Because the activity of NHS-ester may significantly increase at a lower reaction *temperature*, the covalent binding of the GRGDS was performed comparatively at 4 °C (Protocol V) and 25 °C (Protocol VI).[41] However, at 25 °C, an 8% increase in amide I + amide II intensities compared to that in the reaction at 4 °C was observed (see Figure 2). Presumably, the higher diffusion rate of GRGDS at 25 °C results in a better amidation efficiency despite the high hydrolysis rate and short lifetime of NHS-ester with around 4−5 h at 25 °C.[37]

Moreover, the reaction *time* had a significant effect on the bioconjugation efficiency. The covalent GRGDS binding onto PAA brushes according to Protocol VI was performed for 2 h, whereas the bioconjugation lasted 16 h referring to Protocol VII. A significant increase of 39% in amide I + amide II intensities was found for the longer conjugation time.

In conclusion, an overall 78% increase of the bioconjugation efficiency was achieved proceeding from Protocols I to VII. The reaction time had the greatest impact on the chemisorbed GRGDS-peptide amount and was finally fixed at 16 h, for best chemisorption results. The EDC/NHS molar ratio had only a slight effect, whereas the temperature during the covalent binding step strongly influenced the GRGDS conjugation efficiency. The final reaction temperature was 25 °C. The precise selection of solvents and buffers with appropriate pH

DOI: 10.1021/acsomega.6b00450
ACS Omega 2017, 2, 946−958

value and ionic strength played a significant role in each bioconjugation step. In summary, the investigation and comparison of the exemplarily selected seven bioconjugation protocols have evidenced that a precise control of the EDC/NHS chemisorption parameters guarantees a high RGD-peptide conjugation efficiency to polymer brush films.

Figure 2 illustrates the results obtained for the seven protocols in terms of ATR-FTIR spectra (a) and the normalized amide I and amide II band integrals (b). The selected colors of the spectra (a) correspond to those of the normalized amide integral bars (b) as well as to the description of the protocols in Table 2. Importantly, the respective swollen thicknesses were smaller than 80 nm, classifying these films as "thin films" according to Harrick, from which it can be approximated that the measured band integrals are linear to the bound peptide amount (see also above).[43] Conclusively, the GRGDS bioconjugation via EDC/NHS chemisorption Protocol VII could be identified as the most efficient one.

2.4. Analysis of the Optimized GRGDS Peptide Bioconjugation Procedure Using Dynamic in Situ ATR-FTIR. Dynamic in situ ATR-FTIR data describe the chemical composition changes at the polymer brush surface during bioconjugation over a certain time period. With respect to a detailed illustration of the EDC/NHS activation step and the GRGDS conjugation step, in situ ATR-FTIR spectra were subsequently recorded using a liquid cell for the chemisorption, according to Protocol VII (see Section 2.3) for both homo-PAA brushes and PNIPAAm−PAA (80:20) binary brushes analogously.

Figure 3a shows time-dependent in situ ATR-FTIR spectra recorded in the wavenumber region of 1900−1500 cm^{-1} in each surface preparation step of the GRGDS bioconjugation onto the PAA brush surface. The recorded time lapse starts from the bottom gray thick line, continues with the gray thinner lines, and ends up with the red line, which represents the final measurement of each modification step. Each line has a time frame distance of t = 5 min from the next spectrum line. Table 2 summarizes the vibrational band assignments in the focused wavenumber region at the final time point of each examined surface state.

Figure 3a (I) shows the ATR-FTIR spectrum of the PAA brush layer in MES buffer (pH 6). The swelling of the brush was recorded for 15 min to ensure equilibrium. The band at 1729 cm^{-1} is attributed to the C═O stretching vibration of the underlying PGMA layer (ester group). Generally, the PAA brush shows two discrete vibrational bands in the examined region: at 1556 cm^{-1}, where the asymmetric stretching vibration, $\nu_a(COO^-)$, of dissociated COO^- groups appears, and at 1720 cm^{-1}, attributed to the carbonyl stretching vibration, $\nu(C{=}O)$, of protonated COOH groups. The intensity ratio of those signals depends on the degree of protonation of the PAA and thus also on the ionic strength and pH of the solution. The first and last spectra of the dynamic swelling measurements are identical, denoting the instantaneous swelling of the brush layer and nearly full dissociation of the carboxylic acid groups at pH 6.

For the EDC/NHS-activated PAA brush in Figure 3a (II), three new vibrational bands appear: at 1800 cm^{-1}, assigned to NHS-ester; 1761 cm^{-1}, assigned to the carbonyl stretch; and 1732 cm^{-1}, assigned to the symmetric and asymmetric vibrations of the C═O. A slight shift to lower frequencies over time could be seen here for the first 30 min of the measurement, denoting the increased amount of activated carboxylic groups over this time frame. Interestingly, there was no obvious sign of *N*-acylurea and anhydride byproducts during the carboxylic group activation of PAA brush.

The amidation kinetics during chemisorption for 2 h is shown in Figure 3a (III). The NHS-ester band vanishes with time, whereas, simultaneously, the amide I and amide II bands gradually increase at 1660 and 1550 cm^{-1}, respectively, denoting GRGDS-peptide bioconjugation. On a subsequent step, the surface was thoroughly rinsed with PBS, and all loosely bound GRGDS was washed away, whereas the nonreacted NHS-ester was hydrolyzed back to COOH (Figure 3a, IV). Finally, to overcome the overlap of the $\nu_a(COO^-)$ band (1556 cm^{-1}) and the amide II band (1550 cm^{-1}), the surface was quenched with an acetate buffer (pH = 4). Upon protonation of the carboxylic groups, a new carbonyl stretching band ($\nu(C{=}O)$) appeared at 1720 cm^{-1} (Figure 3a, V), which is assigned to COOH groups. As the benefit of this procedure, the spectrum of step (V) shows the quantitatively evaluable amide I and amide II bands without spectral overlap with the PAA bands.

In comparison, Figure 3b shows the ATR-FTIR spectra on the GRGDS bioconjugation onto the PNIPAAm−PAA binary brush. Because of the PNIPAAm component of the binary brush, several additional bands were observed in all taken spectra (Figure 3b, I−V). For instance, the PNIPAAm polymer caused an additional amide I band at 1630 cm^{-1} and an amide II band between 1535 and 1545 cm^{-1}, which further overlaps with the $\nu_a(COO^-)$ band at 1556 cm^{-1} originated from the deprotonation of COOH groups of the PAA component at pH 6. Therefore, both amide bands are more pronounced in all binary brush spectra. Furthermore, in the ATR-FTIR spectra of PNIPAAm−PAA binary brushes, an additional $\nu(CH)$ stretching vibration of the isopropyl groups of PNIPAAm was detected at around 2980 cm^{-1}, which is not shown in the zoomed-in spectra between 1500 and 1900 cm^{-1}.

Summing up, in situ ATR-FTIR was used to analyze the GRGDS bioconjugation process directly at the polymer brush surface on the basis of the dynamic increase and decrease of diagnostic infrared bands. Of particular relevance were the ATR-FTIR spectra after the EDC/NHS activation (II) as well as after the GRGDS conjugation (III). For both polymer brush systems, PAA and PNIPAAm−PAA, no bioconjugation byproducts were detected. Comparing Figure 3a,b (II in both), the relevant bands of the NHS-ester intermediate were less pronounced in the case of binary PNIPAAm−PAA brush activation compared to the homo-PAA brush because of the lower amount of the PAA component (20%) in the former. However, both dynamic conjugation spectra, Figure 3a,b (III in both), prove the successful GRGDS covalent binding to both PAA and PNIPAAm−PAA brushes. While for both systems the NHS-ester bands disappeared, the intensity of the GRGDS-peptide bands, amide I and amide II, increased. After the rinsing step (IV) and the quenching step (V) in Figure 3b, no differences were observed between these corresponding spectra. In contrast to this, a relevant difference between the conjugation spectrum (III), the rinsing spectrum (IV), and the quenching spectrum (V) can be seen in Figure 3a. In case of the homopolymer brush, the washing and quenching procedure resulted obviously in the removal of a certain amount of weakly bound GRGDS and the regeneration of carboxylic groups after the hydrolysis of the unreacted NHS-ester. Finally, the amide I and amide II band intensities after

DOI: 10.1021/acsomega.6b00450
ACS Omega 2017, 2, 946−958

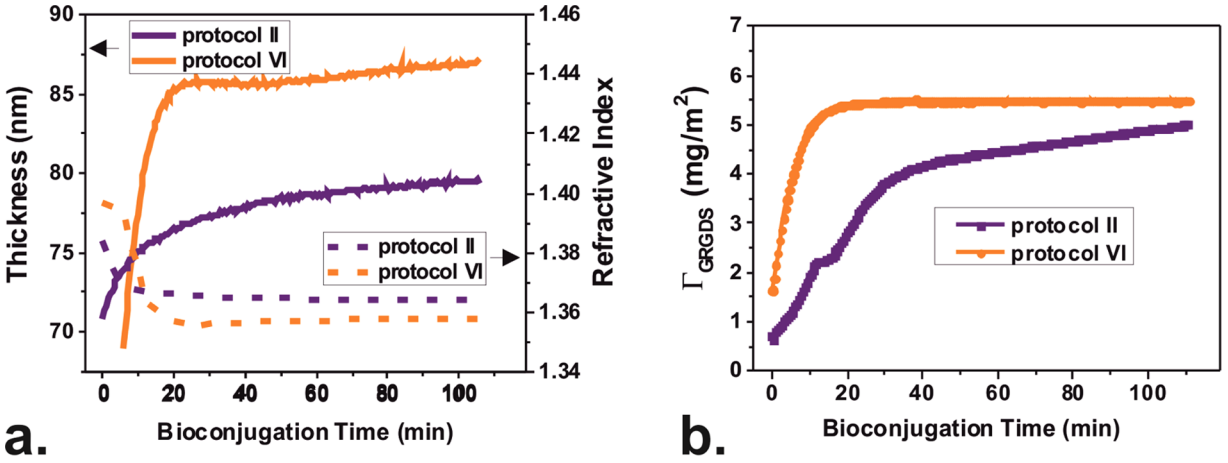

Figure 4. In situ VIS−SE monitoring of GRGDS bioconjugation (0.1 mg/mL) onto homo-PAA brushes. (a) Detection of PAA layer thickness and refractive index changes during bioconjugation. (b) The time-dependent GRGDS amount (mg/m^2) chemisorbed onto the PAA brush surfaces comparing Protocols II and VI. In situ ellipsometry measurements are performed in a batch cell without stirring.

quenching verify the formation of a stable bioconjugation of both polymer brushes.

2.5. In Situ VIS−SE Analysis of GRGDS Bioconjugation. Besides the detailed ATR-FTIR analysis, in situ VIS−SE experiments were carried out to monitor each step of the bioconjugation process performed in the ellipsometry batch cell over time. The ellipsometric study was focused on the monitoring of the GRGDS bioconjugation for about 2 h under optimal conditions regarding Protocol VI in comparison to the less optimized bioconjugation reaction of Protocol II (see Table 2). In general, the experimental parameters of Protocol VI and the final optimized Protocol VII were the same except the longer reaction time of 16 h used for Protocol VII and the absence of shaking for the monitoring of kinetics by in situ ellipsometry.

Initially, the dry PAA brush layer thickness was 8.0 nm. The PAA brush substrate was equilibrated in either 100 mM phosphate (Protocol II) or 100 mM MES (Protocol VI) at pH 6. At this pH, the COOH groups were dissociated, and the PAA brush layer thickness increased with a swelling ratio ($d_{swollen}/d_{dry}$) of approximately 9.0 for all protocols. After the exchange of the buffer against the EDC/NHS activation solution, the PAA brush rapidly collapsed upon reaction of the COO^- groups with EDC/NHS components independent of the EDC/NHS ratio. Once the EDC/NHS solution was substituted by the GRGDS solution, the bioconjugation reaction was initiated. Figure 4a shows the continuous increase of layer thickness and the decrease of refractive index during the GRGDS chemisorption onto homo-PAA brushes with bioconjugation time. During the ellipsometric measurements, the qualitative changes of the PAA brush layer upon the covalent GRGDS binding are influenced by the different bioconjugation temperatures and buffer solutions of Protocols II and VI. In comparison, Figure 4b describes the amount of GRGDS chemisorbed onto the PAA brush surface under the experimental conditions of both protocols. Obviously, the optimized bioconjugation conditions of Protocol VI led to faster changes during the chemisorption reaction and reached a plateau value, whereas the GRGDS bioconjugation according to Protocol II is slower and less effective.

Moreover, additional ellipsometric measurements were carried out to evaluate the influence of different initial GRGDS concentrations (0.05, 0.1, 0.25, and 0.5 mg/mL) on the peptide saturation of the homo-PAA brush layer during 16 h of bioconjugation in the immobilization chamber with additional shaking (see Section 4.4). The experiments were done comparatively under less optimal (Protocol II) and most optimal (Protocol VII) chemisorption conditions, referring to Table 2.

Figure 5 shows the quantitative results of the GRGDS-bioconjugated homo-PAA brush surface. As expected, increasing initial peptide concentrations caused an increasing amount of immobilized GRGDS peptide. The optimal process (Protocol VII (red)) led to about 3-fold higher amounts of bound GRGDS for the same initial peptide concentration, which demonstrates again the higher bioconjugation efficiency of Protocol VII. This is attributed to the higher diffusion rates and consequently the faster chemisorption at 25 °C. Therefore, interactions between GRGDS peptides themselves and between the PAA brush surface and the GRGDS peptide are different for both chemisorption protocols.[37] Figure 5 also illustrates that

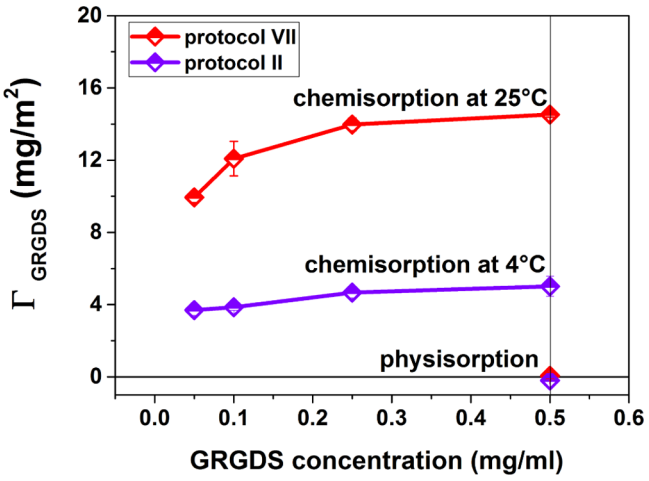

Figure 5. Quantitative VIS−SE analysis of the amount of GRGDS, Γ (mg/m^2), bound to homo-PAA brushes as a function of GRGDS concentration. Comparison of the GRGDS bioconjugation efficiency between the less optimal Protocol II and the most optimal Protocol VII as well as with the GRGDS physisorption results under the same conditions as for conjugation.

DOI: 10.1021/acsomega.6b00450
ACS Omega 2017, 2, 946−958

the biofunctionalization of PAA-containing polymer brushes can be effectively accomplished only by covalent binding of functional GRGDS peptides and not by GRGDS-peptide physisorption. For the Protocol VII and 0.1 mg/mL concentration of GRGDS in solution, a 20% functionalization efficiency of the carboxylic groups can be estimated from the chemisorbed amount of GRGDS (12 mg/m^2) (Figure 2) and the amount of PAA at the surface (7 mg/m^2).

2.6. Analysis of GRGDS Bioconjugation via Acidic Hydrolysis/HPLC. To verify the amounts of GRGDS peptides bioconjugated to polymer brushes as determined by ellipsometry, a chromatographic analysis of the amino acids was performed after the acidic hydrolysis of the surface-bound GRGDS peptide.[29]

Figure 6 shows the surface-bound GRGDS amount after physisorption and chemisorption onto PAA, PNIPAAm−PAA

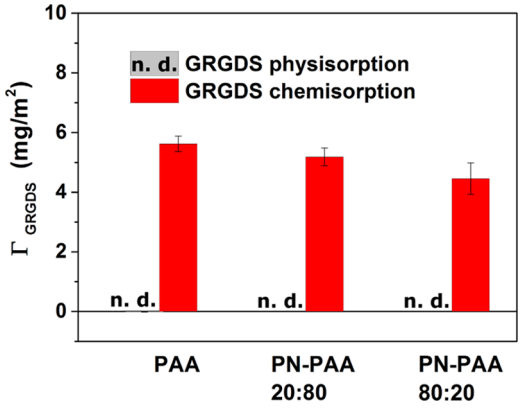

Figure 6. Quantification of the GRGDS peptide bound to a homo-PAA brush and to binary PNIPAAm−PAA brushes with ratios 20:80 and 80:20 by acidic hydrolysis and subsequent HPLC analysis. Comparison of physisorption and chemisorption following the optimized Protocol VII. Initial GRGDS concentration was 0.1 mg/mL. The physisorbed amounts were below the detection limit (n.d.).

(PN−PAA) 20:80, and PNIPAAm−PAA 80:20 polymer brushes using an initial GRGDS peptide concentration of 0.1 mg/mL. On the one hand, it was proved that upon physisorption, almost no GRGDS was adsorbed to any of the investigated PAA-containing polymer brushes (Figure 6, light gray column). On the other hand, GRGDS was successfully chemisorbed to the PAA component of the brush using Protocol VII (Figure 6, red column). The GRGDS amount chemisorbed to the binary brushes decreased with their PAA concentration: 5.6 mg/m^2 (homo-PAA) > 5.2 mg/m^2 (binary PN−PAA 20:80) > 4.5 mg/m^2 (PN−PAA 80:20). However, this decrease was smaller than the decrease of the PAA concentration in the binary brushes from 80 to 20%. It seems that dilution of the PAA chains by PNIPAAm improves the accessibility of the PAA chains and the carboxylic acid group for bioconjugation. The binary brush PNIPAAm−PAA 80:20 will be a promising candidate for further conformational considerations with respect to a possible spatial GRGDS arrangement, which is important for cell-responsive studies.

Notably, the HPLC calculated amount, Γ_{GRGDS}, is in the same range but not in an absolute agreement with the modeled VIS−SE data (see Section 2.5). We assume that a considerable amount of peptide has been absorbed either on the walls or on the underlying surface of the incubator (Petri dish microplates) or washed away. Consequently, the efficiency of the conjugation (feed vs obtained) in case of the HPLC analysis was found to be low (7.5% for PAA polymer surface).

3. CONCLUSIONS

This study aimed at a detailed understanding of the interfacial bioconjugation of the RGD-peptide GRGDS with polymer brush coatings in the context of designing nanoscale biointerfaces with versatile biomedical cues. Two homopolymer brushes, PAA and PNIPAAm, and a two binary polymer brush system (PNIPAAm−PAA) prepared by the *grafting-to* approach were used. The pentapeptide, GRGDS, was bound via physisorption or chemisorption. As the main research issue, in situ monitoring of the GRGDS bioconjugation was addressed by complementary analytical techniques such as in situ ATR-FTIR, in situ VIS−SE, and acid hydrolysis/HPLC analyses.

Because it was shown that the GRGDS physisorption on all tested brush coatings was minimal, chemisorption of GRGDS was mandatory.

Hence, GRGDS was covalently bound to the PAA component on the basis of the carboxyl-to-amine bioconjugation using EDC and NHS simultaneously. In situ monitoring of the chemisorption steps by ATR-FTIR analysis revealed the influence of experimental parameters, such as the chosen buffer, reaction time, and temperature, and led to the identification of optimal conditions as 100 mM MES buffer at pH 6 for activation and 100 mM borate buffer at pH 8, 16 h, and T = 25 °C for conjugation. This method, which is sensitive to chemical changes at the interface, delivered information about successful PAA activation as well as via changes of the band intensities of NHS-ester and amide I and amide II, a confirmation of the effectiveness of the GRGDS bioconjugation.

Complementarily, in situ VIS−SE measurements provided brush thicknesses and adsorbed GRGDS amounts, which were verified by direct quantitative amino acid analysis using acidic hydrolysis and subsequent HPLC analysis, as an additional measure of the effectiveness of the bioconjugation process. On the basis of these findings, a thermoresponsive PNIPAAm−PAA binary brush with a ratio of 80:20 functionalized with a considerably high amount of GRGDS peptide was produced. This system is expected to have a specific relevance for temperature-responsive GRGDS presentation at the brush surface for further investigations, such as cell-instructive studies. In summary, the reported bioconjugation approach shown exemplarily for GRGDS paves the way for manifold applications of polymer brush platforms in bioscience, bioengineering, and bionanotechnology, where the surface-induced modulation of cellular functions, such as adhesion, spreading, migration, proliferation, and cytoskeletal organization, is required.

4. EXPERIMENTAL PROCEDURES

4.1. Materials. PGMA (M_n = 17 500 g/mol, M_w/M_n = 1.7), PAA (M_n = 25 000 g/mol, M_w/M_n = 1.2), and carboxy-terminated PNIPAAm (M_n = 42 000 g/mol, M_w/M_n = 1.2) were purchased from Polymer Source, Inc., Canada. Ethanol absolute, chloroform ($CHCl_3$), and acetic acid were obtained from VWR, Fisher, and Merck (all Germany), respectively. PBS (tablets, pH 7.4), EDC, NHS, potassium phosphate dibasic trihydrate, sodium phosphate dibasic dihydrate, sodium hydroxide, boric acid, and MES were purchased from Sigma-Aldrich (Germany). Fibronectin active fragment Gly-Arg-Gly-

DOI: 10.1021/acsomega.6b00450
ACS Omega 2017, 2, 946−958

Asp-Ser (GRGDS) was obtained from Peptides International Inc. (Louisville, KY and Canada). Silicon wafers oriented in [100] direction and with 2 nm native SiO_2 layer from Si-Mat (Landsberg, Germany) were used as substrates.

4.2. Preparation of Polymer Brushes. Polymer brushes were prepared by the *grafting-to* method according to previously published work.[7,25,26] Briefly, silicon wafer pieces (size 1.3 cm × 2 cm) were cleaned with ethanol by ultrasonication and subsequently activated in an oxygen plasma chamber (1 min at 100 W). To prepare anchoring layers for the brush polymers on the silicon substrates, PGMA solution (0.02 wt % in chloroform) was spin-coated and annealed at 100 °C under vacuum for 20 min, resulting in a thin reactive layer with epoxy groups for the following *grafting-to* step. A second polymer solution consisting of PAA (1 wt % in ethanol) was spin-coated and annealed at 80 °C for 30 min. The nongrafted polymer was removed by washing the samples in ethanol for 20 min and drying them with a N_2 flux. The procedure led to the fabrication of PAA homopolymer pseudobrushes, where the polymers are grafted with more than one anchoring point to the surface, forming loops and tails. These layers behave similarly to polymer brushes as the number of anchoring points (n) is between 1 and 2 and the swelling ratio is comparable to the swelling ratio of a PAA brush made by end-tethered polymers.[45,46] For the preparation of PNIPAAm homopolymer brushes, a solution of carboxy-terminated PNIPAAm (1 wt% in chloroform) was spin-coated on the PGMA layer and subsequently annealed at 150 °C overnight. The unbound polymer was extracted in water for 4 h, and the brushes were finally dried by a N_2 flux. For the preparation of binary brushes, carboxy-terminated PNIPAAm (1 wt% in chloroform) was initially spin-coated and annealed at different time intervals to achieve different grafted amounts of PNIPAAm. After extraction with water, PAA was grafted to the surface in the same manner as for the homopolymer brush. The composition of the binary brushes was determined by the ratio of the subsequent polymer layer thickness determined by ellipsometry.[7] A detailed physicochemical analysis of particular polymer brushes was published previously.[26,45]

4.3. Biofunctionalization of Polymer Brushes with RGD Peptides. Both physisorption and chemisorption of RGD peptides onto polymer brushes were carried out by using a home-built immobilization chamber designed by König.[47] For physisorption, GRGDS in buffer solution was adsorbed overnight onto primarily swollen polymer brush surfaces under gentle stirring. The adsorption on PNIPAAm brushes was performed with PBS buffer (pH = 7.4) at different temperatures (25 or 40 °C), lower and higher than the LCST of PNIPAAm (around 32 °C). The physisorption on PAA brushes was done in buffers with varied pH values at 25 °C. For pHs 5 and 6, a 100 mM sodium acetate buffer was used, and for pHs 7 and 8, a 100 mM sodium phosphate buffer was used. GRGDS solutions were prepared with the following concentrations: 0.05, 0.1, 0.25, and 0.5 mg/mL.

For the bioconjugation process via EDC/NHS, we investigated several experimental reaction parameters, such as the concentration and molar ratio of the activation and conjugation reagents, buffer characteristics, activation and conjugation times, and temperatures, and the final washing steps on the GRGDS-peptide conjugation efficiency. Table 3 gives a general overview of the investigated chemisorption parameters. For all experiments illustrated in the following figures, the GRGDS-peptide concentration of 0.1 mg/mL was used.

Table 3. Summary of All Comparatively Investigated Reaction Parameters Tested for the GRGDS Bioconjugation via EDC/NHS Chemisorption

	activation (A)	
parameters	method A-I	method A-II
activation buffer	100 mM MES; pH 6	100 mM phosphate; pH 6
EDC/NHS molar ratio	2.5/1 vs 1/2.5	2.5/1 vs 1/2.5
temperature	25 °C	25 °C
activation time	30 min to 2 h	30 min to 2 h
rinsing	no rinsing vs with MES buffer	no rinsing vs with phosphate buffer
	covalent binding (B)	
parameters	method B-I	method B-II
conjugation buffer	100 mM borate, pH 8	100 mM PBS; pH 7.4
temperature	4 vs 25 °C	4 vs 25 °C
conjugation time	30 min to 16 h	30 min to 16 h
rinsing	1. thorough washing with PBS	
	2. quenching with acetate buffer; pH 4	

In detail, for the most optimal Protocol VII of Table 2, the following steps were performed. Before the activation procedure, the polymer brush surface was incubated with 1 mL of MES buffer (pH 6; 100 mM) for 10 min. Then, the surface was aspirated, and 1 mL of EDC/NHS (molar ratio, 1:2.5) was added for 30 min to activate the COOH groups. For the covalent binding, the surface was aspirated, and 0.1 mg/mL GRGDS in borate buffer (pH 8; 100 mM) was added; chemisorption was performed for 16 h under shaking. EDC/NHS was provided in large excess (μmol) compared to the amount of carboxylic groups (nmol) at the PAA chains. The surface was thoroughly washed with PBS buffer before analytical testing.

4.4. Surface Characterization Methods. *4.4.1. ATR-FTIR.* ATR-FTIR spectra were recorded on a BRUKER TENSOR 27 spectrometer (Bruker Optics GmbH, Ettlingen, Germany) equipped with a dedicated in situ ATR-FTIR device (OPTISPEC, Zürich, Switzerland). In situ ATR-FTIR flow cells (custom made) with four separated liquid compartments on the lower and upper halves of the front and rear housing trapezoidal internal reflection elements (IRE, KOMLAS GmbH, Berlin) of silicon (Si) with dimensions 50 × 20 × 2 mm^3 allowing incident angles (θ) of 45° were used. For the ATR-FTIR experiments, a dedicated optical ATR attachment operating by the "single-beam-sample reference" (SBSR) concept (OPTISPEC, Zürich, Switzerland) was used on the basis of a recording sample (silicon/polymer, I_S) and a reference (silicon) intensity (I_R) quasi-simultaneously by shuttling the upper (sample) and lower halves (reference) of the Si-IRE separately into the IR beam (lift). Relating I_S to I_R results in well-compensated ATR-FTIR absorbance spectra according to $A = -\log(I_S/I_R)$.

In detail, after a thorough cleaning of the Si-IRE by plasma cleaning under reduced air pressure (Plasma Cleaner, Harrick, Ossining), the Si-IRE was first coated by anchoring a PGMA layer according to the protocol given above on the full front side. Thereafter, the lower half (50 × 10 × 2 mm^3) of the Si-IRE was thoroughly cleaned using a folded soft tissue soaked in ethanol, and the corresponding ATR-FTIR spectrum of PGMA was recorded. In the second step, the PAA or PNIPAAm−PAA

DOI: 10.1021/acsomega.6b00450
ACS Omega 2017, 2, 946−958

brush was *grafted to* this PGMA layer according to the protocol given above, and the corresponding PGMA/brush ATR-FTIR spectrum was recorded. The same procedure was applied for the activation step, the GRGDS-peptide binding step, and further steps. The ATR-FTIR spectra of actual total layer assemblies were obtained by subtracting the spectrum of bare Si-IRE, whereas those of the corresponding actual top layers (e.g., bound RGD peptide) could be obtained by subtracting the spectrum of the respective underlying layer assemblies. The samples were analyzed in either the dry state or the wet state, where after each modification step the compartments were either purged by N_2 or filled with respective aqueous medium. Measurements after each step were performed after an equilibration time of 10 min. Experimental analysis was performed using OPUS software (version 7.0) supplied by BRUKER Optics GmbH (Ettlingen, Germany).

4.4.2. In Situ Spectroscopic Ellipsometry (VIS−SE). The in situ ellipsometric setup for measurements on highly swellable polymer brushes and subsequent biomolecule conjugation as well as modeling of these systems has been reviewed recently.[48] In the present study, a spectroscopic ellipsometer equipped with a rotating compensator (α-SE; Woollam Co., Inc., Lincoln NE) was used. The ellipsometric data, Δ (relative phase shift) and $\tan\Psi$ (relative amplitude ratio), were recorded at wavelengths within the visible optical range of 400−800 nm. The angle of incidence (Φ_0) was kept constant at 70°, close to the Brewster angle of silicon. All data were acquired and analyzed using Complete EASE software, version 4.46. The in situ measurements for the investigation of the peptide conjugation were performed in different buffers at 25 °C using a quartz cuvette (TSL Spectrosil, Hellma, Muellheim, Germany). The wafers were kept fixed in the cuvette by a home-built Teflon holder.

The ellipsometric modeling of the polymer brushes was based on a multilayer box model with distinct interfaces consisting of silicon, silicon dioxide, anchoring layer PGMA, and the polymer brush to evaluate the refractive index (n) as well as dry and swollen brush thickness (d) of the layers. The optical dispersion relations for silicon and silicon oxide were taken from the software library, and the refractive index of PGMA was set to $n_{(PGMA)} = 1.525$. The dependence of the refractive index on the wavelength was described by the Cauchy relation: $n(\lambda) = A + B/\lambda^2$. In case of very thin ($d < 10$ nm), dry brush films, the Cauchy parameters, A and B, were modeled from measurements of a 50 nm thick dry polymer layer and applied as fixed values in the Cauchy relation. The extinction coefficients, $k(\lambda)$, of the PGMA and brushes are zero in the measured spectral range.

Modeling RGD-peptide adsorption on swollen, soft polymer brush films from ellipsometric data requires different analysis models than for smooth, rigid surfaces because of the increased complexity of the RGD-brush system. No sharp interface between the peptide and the polymer brush is present, and the peptide is assumed to penetrate into the PEL brush layer. Thus, a composite polymer−peptide box layer is modeled, resulting in an average Cauchy dispersion for both components, which does not differentiate between the incorporation mode (primary: onto the PGMA layer; secondary: at the brush−solution interface; or ternary: along the polymer chains). The resulting parameters of the model are a combined in situ layer thickness (d_{comb}) and the average dispersion relation ($n_{comb}(\lambda)$). To determine the GRGDS-peptide amount chemisorbed onto the brush surface, a modified de Feijter equation was used.

$$\Gamma_{GRGDS} = d_{brush}\frac{n_{comb} - n_{brush}}{\left(\frac{dn}{dc}\right)_{GRGDS}} + d_{add}\frac{n_{comb} - n_{amb}}{\left(\frac{dn}{dc}\right)_{GRGDS}} \quad (1)$$

Here, d_{brush} and n_{brush} are the parameters of the swollen brush layer before adsorption, n_{amb} is the refractive index of the ambient solution, and $(dn/dc)_{GRGDS} = 0.185$ cm^3/g is the refractive index increment of the peptide, averaged over the individual amino acids.[49] The relation $d_{add} = d_{comb} - d_{brush}$ accounts for changes in the layer thickness due to the adsorption process. It can be shown that eq 1 is valid for d_{add} positive or negative and represents a virtual two-layer approach for calculation only. Changes in the brush conformation upon adsorption do not have to be regarded directly, given that the amount of brush polymer stays constant at the surface. Typically, n (λ = 633 nm) was chosen for the calculations.

4.4.3. Acidic Hydrolysis and Subsequent HPLC. Quantification of the bioconjugated GRGDS, which was either physisorbed or chemisorbed on polymer brushes, was performed by acidic hydrolysis of the surface-bound peptide sequence and subsequent reverse-phase HPLC analysis of the amino acids, as described in Salchert et al. in detail.[29] Therefore, GRGDS-functionalized polymer brushes were first subjected to vapor-phase hydrolysis in vacuum using 6 M HCl at 110 °C for 24 h and subsequent neutralization. The extraction of amino acids from the samples was accomplished by repeated rinsing with a definite volume of 50 mM sodium acetate buffer at pH 6.8. A defined volume of this extract was injected into the HPLC system (Agilent 1100 LC), and the dissolved amino acids were chromatographically separated after precolumn derivatization with ortho-phthalaldehyde (Sigma-Aldrich) on a Zorbax SBC18 column (4.6 × 150 mm^2, 3.5 μm, Agilent Technologies, Boeblingen, Germany) followed by a fluorescence detection (excitation wavelength of 335 nm, emission measured at 455 nm). At least two empty glass tubes without samples were checked in parallel to give a blank value. After calibration with an amino acid standard for fluorescence detection (Sigma-Aldrich, Germany), the HPLC peaks (area) of aspartic acid, serine, glycine, and arginine were evaluated to calculate the mass of GRGDS in the injected volume. From this, the surface concentration of GRGDS (in mg/m^2) was obtained by taking into account the ratio of the injected volume to the total volume of the amino acid extract and the surface area of the silicon wafer pieces (1.3 × 2 cm^2) and, if necessary, dilution factors.

AUTHOR INFORMATION

Corresponding Authors

*E-mail: koenig-ulla@ipfdd.de (U.K.).
*E-mail: uhlmannp@ipfdd.de (P.U.).

ORCID

Petra Uhlmann: 0000-0001-9298-4083

Author Contributions

‖E.P. and U.K. contributed equally to this work.

Funding

This work was supported by the DFG grants STA 324/49-1 and EI 317.

Notes

The authors declare no competing financial interest.

DOI: 10.1021/acsomega.6b00450
ACS Omega 2017, 2, 946−958

■ ACKNOWLEDGMENTS

The authors acknowledge German Academic Exchange Service (DAAD) and particularly the RISE program. Special thanks go to Argyro Spinthaki, who performed the RGD-peptide physisorption on PNIPAAm brushes within this program. The authors also thank their partners within a joint project in the frame of "Materials Word Network" funded by DFG and NSF for fruitful discussions. In particular, they thank Milauscha Grimmer for the diligent HPLC performance and analysis. Special thanks also go to Carolin Böhm, who supported the polymer brush fabrication and analysis.

■ REFERENCES

(1) Hynes, R. O. Integrins: a family of cell surface receptors. *Cell* **1987**, *48*, 549−554.
(2) Pierschbacher, M. D.; Ruoslahti, E. Cell attachment activity of fibronectin can be duplicated by small synthetic fragments of the molecule. *Nature* **1984**, *309*, 30−33.
(3) Delaittre, G.; Greiner, A. M.; Pauloehrl, T.; Bastmeyer, M.; Barner-Kowollik, C. Chemical approaches to synthetic polymer surface biofunctionalization for targeted cell adhesion using small binding motifs. *Soft Matter* **2012**, *8*, 7323−7347.
(4) Luo, Y.; Shoichet, M. S. A photolabile hydrogel for guided three-dimensional cell growth and migration. *Nat. Mater.* **2004**, *3*, 249−253.
(5) Grafahrend, D.; Heffels, K.-H.; Beer, M. V.; Gasteier, P.; Möller, M.; Boehm, G.; Dalton, P. D.; Groll, J. Degradable polyester scaffolds with controlled surface chemistry combining minimal protein adsorption with specific bioactivation. *Nat. Mater.* **2011**, *10*, 67−73.
(6) Alves, N. M.; Pashkuleva, I.; Reis, R. L.; Mano, J. F. Controlling cell behavior through the design of polymer surfaces. *Small* **2010**, *6*, 2208−2220.
(7) Minko, S.; Patil, S.; Datsyuk, V.; Simon, F.; Eichhorn, K.-J.; Motornov, M.; Usov, D.; Tokarev, I.; Stamm, M. Synthesis of adaptive polymer brushes via "grafting to" approach from melt. *Langmuir* **2002**, *18*, 289−296.
(8) Lemieux, M.; Usov, D.; Minko, S.; Stamm, M.; Shulha, H.; Tsukruk, V. V. Reorganization of binary polymer brushes: Reversible switching of surface microstructures and nanomechanical properties. *Macromolecules* **2003**, *36*, 7244−7255.
(9) Stuart, M. A. C.; Huck, W. T.; Genzer, J.; Müller, M.; Ober, C.; Stamm, M.; Sukhorukov, G. B.; Szleifer, I.; Tsukruk, V. V.; Urban, M. Emerging applications of stimuli-responsive polymer materials. *Nat. Mater.* **2010**, *9*, 101−113.
(10) Krishnamoorthy, M.; Hakobyan, S.; Ramstedt, M.; Gautrot, J. E. Surface-initiated polymer brushes in the biomedical field: applications in membrane science, biosensing, cell culture, regenerative medicine and antibacterial coatings. *Chem. Rev.* **2014**, *114*, 10976−11026.
(11) Jiang, H.; Xu, F.-J. Biomolecule-functionalized polymer brushes. *Chem. Soc. Rev.* **2013**, *42*, 3394−3426.
(12) Ebara, M.; Yamato, M.; Aoyagi, T.; Kikuchi, A.; Sakai, K.; Okano, T. The effect of extensible PEG tethers on shielding between grafted thermo-responsive polymer chains and integrin−RGD binding. *Biomaterials* **2008**, *29*, 3650−3655.
(13) Li, L.; Wu, J.; Gao, C. Gradient immobilization of a cell adhesion RGD peptide on thermal responsive surface for regulating cell adhesion and detachment. *Colloids Surf., B* **2011**, *85*, 12−18.
(14) Navarro, M.; Benetti, E. M.; Zapotoczny, S.; Planell, J. A.; Vancso, G. J. Buried, covalently attached RGD peptide motifs in poly (methacrylic acid) brush layers: the effect of brush structure on cell adhesion. *Langmuir* **2008**, *24*, 10996−11002.
(15) Hopwood, D. A comparison of the crosslinking abilities of glutaraldehyde, formaldehyde and α-hydroxyadipaldehyde with bovine serum albumin and casein. *Histochem. Cell Biol.* **1969**, *17*, 151−161.
(16) Kiernan, J. A. Formaldehyde, formalin, paraformaldehyde and glutaraldehyde: what they are and what they do. *Microsc. Today* **2000**, *1*, 8−12.
(17) Harris, B. P.; Kutty, J. K.; Fritz, E. W.; Webb, C. K.; Burg, K. J.; Metters, A. T. Photopatterned polymer brushes promoting cell adhesion gradients. *Langmuir* **2006**, *22*, 4467−4471.
(18) Kutnyanszky, E.; Vancso, G. J. Nanomechanical properties of polymer brushes by colloidal AFM probes. *Eur. Polym. J.* **2012**, *48*, 8−15.
(19) Choi, W. S.; Bae, J. W.; Lim, H. R.; Joung, Y. K.; Park, J.-C.; Kwon, I. K.; Park, K. D. RGD peptide-immobilized electrospun matrix of polyurethane for enhanced endothelial cell affinity. *Biomed. Mater.* **2008**, *3*, No. 044104.
(20) Wang, C.; Yan, Q.; Liu, H.-B.; Zhou, X.-H.; Xiao, S.-J. Different EDC/NHS activation mechanisms between PAA and PMAA brushes and the following amidation reactions. *Langmuir* **2011**, *27*, 12058−12068.
(21) Steffens, G.C.M.; Nothdurft, L.; Buse, G.; Thissen, H.; Höcker, H.; Klee, D. High density binding of proteins and peptides to poly (D, L-lactide) grafted with polyacrylic acid. *Biomaterials* **2002**, *23*, 3523−3531.
(22) Sehgal, D.; Vijay, I. K. A method for the high efficiency of water-soluble carbodiimide-mediated amidation. *Anal. Biochem.* **1994**, *218*, 87−91.
(23) Sam, S.; Touahir, L.; Salvador Andresa, J.; Allongue, P.; Chazalviel, J.-N.; Gouget-Laemmel, A.; Henry de Villeneuve, C.; Moraillon, A.; Ozanam, F.; Gabouze, N. Semiquantitative study of the EDC/NHS activation of acid terminal groups at modified porous silicon surfaces. *Langmuir* **2010**, *26*, 809−814.
(24) Psarra, E. Biofunctionalization of Polymer Brush Surfaces. Thesis, Technische Universität Dresden, Germany, 2015.
(25) Psarra, E.; Foster, E.; König, U.; You, J.; Ueda, Y.; Eichhorn, K.-J.; Müller, M.; Stamm, M.; Revzin, A.; Uhlmann, P. Growth Factor-Bearing Polymer Brushes - Versatile Bioactive Substrates Influencing Cell Response. *Biomacromolecules* **2015**, *16*, 3530−3542.
(26) Psarra, E.; König, U.; Ueda, Y.; Bellmann, C.; Janke, A.; Bittrich, E.; Eichhorn, K.-J.; Uhlmann, P. Nanostructured Biointerfaces: Nanoarchitectonics of Thermoresponsive Polymer Brushes Impact Protein Adsorption and Cell Adhesion. *ACS Appl. Mater. Interfaces* **2015**, *7*, 12516−12529.
(27) Burkert, S.; Bittrich, E.; Kuntzsch, M.; Müller, M.; Eichhorn, K.-J.; Bellmann, C.; Uhlmann, P.; Stamm, M. Protein resistance of PNIPAAm brushes: application to switchable protein adsorption. *Langmuir* **2010**, *26*, 1786−1795.
(28) Xue, C.; Yonet-Tanyeri, N.; Brouette, N.; Sferrazza, M.; Braun, P. V.; Leckband, D. E. Protein adsorption on poly(N-isopropylacrylamide) brushes: dependence on grafting density and chain collapse. *Langmuir* **2011**, *27*, 8810−8818.
(29) Salchert, K.; Pompe, T.; Sperling, C.; Werner, C. Quantitative Analysis of Immobilized Proteins and Protein Mixtures by Amino Acid Analysis. *J. Chromatogr. A* **2003**, *1005*, 113−122.
(30) Czeslik, C.; Jackler, G.; Hazlett, T.; Gratton, E.; Steitz, R.; Wittemann, A.; Ballauff, M. Salt-induced protein resistance of polyelectrolyte brushes studied using fluorescence correlation spectroscopy and neutron reflectometry. *Phys. Chem. Chem. Phys.* **2004**, *6*, 5557.
(31) Wittemann, A.; Haupt, B.; Ballauff, M. Adsorption of proteins on spherical polyelectrolyte brushes in aqueous solution. *Phys. Chem. Chem. Phys.* **2003**, *5*, 1671−1677.
(32) de Vos, W. M.; Biesheuvel, P. M.; de Keizer, A.; Kleijn, J. M.; Cohen Stuart, M. A. Adsorption of the Protein Bovine Serum Albumin in a Planar Poly(acrylic acid) Brush Layer As Measured by Optical Reflectometry. *Langmuir* **2008**, *24*, 6575−6584.
(33) Iwasawa, T.; Wash, P.; Gibson, C.; Rebek, J. Reaction of an Introverted Carboxylic Acid with Carbodiimide. *Tetrahedron* **2007**, *63*, 6506−6511.
(34) Müller, M.; Keßler, B.; Houbenov, N.; Bohata, K.; Pientka, Z.; Brynda, E. pH Dependence and Protein Selectivity of Poly-(ethyleneimine)/Poly(acrylic acid) Multilayers Studied by in Situ ATR-FTIR Spectroscopy. *Biomacromolecules* **2006**, *7*, 1285−1294.

DOI: 10.1021/acsomega.6b00450
ACS Omega 2017, 2, 946−958

(35) Müller, M.; Torger, B.; Bittrich, E.; Kaul, E.; Ionov, L.; Uhlmann, P.; Stamm, M. In-situ ATR-FTIR for Characterization of Thin Biorelated Polymer Films. *Thin Solid Films* **2014**, *556*, 1−8.
(36) Burkert, S.; Müller, M.; Uhlmann, P.; Stamm, M. Sensitive Swelling and Controlled Protein Adsorption on Thin Polymer Brush Layers. *Macromol. React. Eng.* **2007**, *1*, F25−F26.
(37) Hermanson, G. T. *Bioconjugate Techniques*, 3rd ed.; Academic Press, 2013.
(38) Vashist, S. K. Comparison of 1-ethyl-3-(3-dimethylaminopropyl) carbodiimide based strategies to crosslink antibodies on amine-functionalized platforms for immunodiagnostic applications. *Diagnostics* **2012**, *2*, 23−33.
(39) Fischer, M. J. E. Amine Coupling through EDC/NHS: A Practical Approach. In *Surface Plasmon Resonance*; Mol, N. J., Fischer, M. J. E., Eds.; Methods in Molecular Biology; Humana Press, 2010; Vol. *627*, pp 55−73.
(40) Bentzen, E. L.; Tomlinson, I. D.; Mason, J.; Gresch, P.; Warnement, M. R.; Wright, D.; Sanders-Bush, E.; Blakely, R.; Rosenthal, S. J. Surface modification to reduce nonspecific binding of quantum dots in live cell assays. *Bioconjugate Chem.* **2005**, *16*, 1488−1494.
(41) Bartczak, D.; Kanaras, A. G. Preparation of peptide-functionalized gold nanoparticles using one pot EDC/sulfo-NHS coupling. *Langmuir* **2011**, *27*, 10119−10123.
(42) de los Santos Pereira, A.; Riedel, T.; Brynda, E.; Rodriguez-Emmenegger, C. Hierarchical antifouling brushes for biosensing applications. *Sens. Actuators, B* **2014**, *202*, 1313−1321.
(43) Harrrick, N. J.; Beckmann, K. H. Internal Reflection Spectroscopy. In *Characterization of Solid Surfaces*; Kane, P. F., Larrabee, G. B., Ed.; Plenum Press: New York, 1974; pp 215−245.
(44) Lin-Vien, D.; Colthup, N. B.; Fateley, W. G.; Grasselli, J. G. *The Handbook of Infrared and Raman Characteristic Frequencies of Organic Molecules*; Academic Press, 1991.
(45) Bittrich, E.; Rodenhausen, K. B.; Eichhorn, K.-J.; Hofmann, T.; Schubert, M.; Stamm, M.; Uhlmann, P. Protein adsorption on and swelling of polyelectrolyte brushes: A simultaneous ellipsometry-quartz crystal microbalance study. *Biointerphases* **2010**, *5*, 159−167.
(46) Guiselin, O. Irreversible adsorption of a concentrated polymer solution. *Europhys. Lett.* **1992**, *17*, 225.
(47) König, U. Molekulare Grenzschichtgestaltung zur Verbesserung der Blutkompatibilität von Polytetrafluorethylen. Thesis, Technische Universität Dresden, Germany, 2000.
(48) Bittrich, E.; Uhlmann, P.; Eichhorn, K.-J.; Hinrichs, K.; Aulich, D.; Furchner, A. Polymer Brushes, Hydrogels, Polyelectrolyte Multilayers: Stimuli-Responsivity and Control of Protein Adsorption. In *Ellipsometry of Functional Organic Surfaces and Films*; Hinrichs, K., Eichhorn, K.-J., Eds.; Springer Series in Surface Sciences; Springer-Verlag: Berlin, 2014; pp 79−105.
(49) Zhao, H.; Brown, P. H.; Schuck, P. On the distribution of protein refractive index increments. *Biophys. J.* **2011**, *100*, 2309−2317.

DOI: 10.1021/acsomega.6b00450
ACS Omega 2017, 2, 946−958